International Conference on Space Optics—ICSO 2008

Toulouse, France

14–17 October 2008

Edited by Josiane Costeraste, Errico Armandillo, and Nikos Karafolas

Instrumental concept and preliminary performances of SIFTI: static infrared fourier transform interferometer

Philippe-Jean Hébert

E. Cansot

C. Pierangelo

C. Buil

et al.

esa icso proceedings cnes

International Conference on Space Optics — ICSO 2008, edited by Josiane Costeraste, Errico Armandillo, Nikos Karafolas, Proc. of SPIE Vol. 10566, 1056623 · © 2008 ESA and CNES
CCC code: 0277-786X/17/$18 · doi: 10.1117/12.2308253

INSTRUMENTAL CONCEPT AND PRELIMINARY PERFORMANCES OF SIFTI: STATIC INFRARED FOURIER TRANSFORM INTERFEROMETER

P. Hébert[(1)], E. Cansot[(1)], C. Pierangelo[(1)], C. Buil[(1)], F. Bernard[(1)], J. Loesel[(1)], T. Trémas[(1)], L. Perrin[(1)], E. Courau[(1)], C. Casteras[(1)], I. Maussang[(1)], D. Simeoni[(2)]

[(1)] Centre National d'Etudes Spatiales, 18 av. E. Belin, 31401 Toulouse Cedex (France), philippe-jean.hebert@cnes.fr
Thales Alenia Space – France, 100 bd du Midi – BP 99, 06156 Cannes la Bocca Cedex (France), denis.simeoni@thalesaleniaspace.com

ABSTRACT

The SIFTI (Static Infrared Fourier Transform Interferometer) instrument aims at supporting an important part in a mission for atmospheric pollution sounding from space, by providing high spectral resolution and high Signal to Noise Ratio spectra of the atmosphere. They will allow to resolve tropospheric profiles of ozone (O_3) and carbon monoxide (CO), especially down to the planetary boundary layer (PBL), an altitude region of very high interest, though poorly monitored to date, for air quality and pollution monitoring. The retrieved profile of ozone, resp. CO, will contain 5 to 7, resp. 2.5 to 4, independent pieces of information.

The French space agency CNES (Centre National d'Etudes Spatiales) has proposed and is studying an instrument concept for SIFTI based on a static interferometer, where the needed optical path are generated by a pair of crossed staircase fixed mirrors (replacing the moving reflector of dynamic Fourier transform interferometers like IASI or MIPAS). With the SIFTI design, a very high spectral resolution (~0.1 cm^{-1} apodised) is achieved in a very compact optical setup, allowing a large throughput, hence a high SNR. The measurements are performed in the 9.5 µm band for O_3 and in the 4.6 µm band for CO.

The science return of the sounder can be further increased if an "intelligent pointing" process is implemented. This consists in combining the TIR sounder with a companion TIR imager, providing information on the cloud coverage in the next observed scene. Onboard, real-time analysis of the IR image is used to command the sounder staring mirror to cloud free areas, which will maximize the probability for probing down to the surface.

After the first part of the phase A, the architecture of SIFTI was studied as a trade-off between performance and resource budget. We review the main architecture and functional choices, and their advantages. The preliminary instrument concept is then presented in its main aspects and in terms of main subsystem functions.

The preliminary budgets of mass, volume, size and power are also evaluated. Eventually the science performances are estimated, at instrument level and at mission level, and are compared to the specifications. To finish, the ways forward are discussed.

1. INSTRUMENT CONCEPT

The principle of static interferometry relies on a CNES patented concept: the moving mirror of classical Michelson interferometers is replaced by a static stepped mirror. Thus temporal acquisition of the interferogram is replaced by spatial acquisition onto a detector matrix (see Fig. 1).

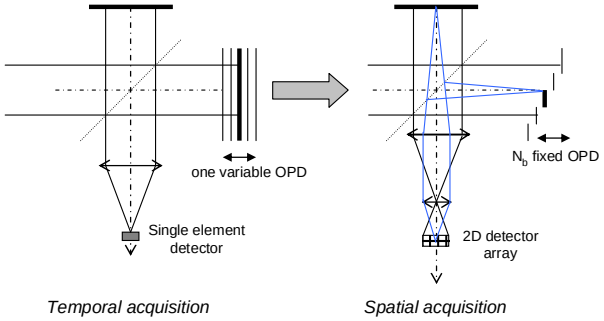

Fig. 1.: from dynamic FTS to static FTS.

The spectral non apodized resolution is given by $\delta\sigma = \frac{1}{2.\text{maximum OPD}}$ as in any type of interferometer, but with no moving (scanning) mirror, which is the main advantage of static interferometry in terms of reliability and dynamic perturbations.

A two dimension array of OPD (Optical Path Difference) facets are obtained by crossing the steps of the stepped mirrors of both arms of the interferometer, such as those presented in Fig. 2:

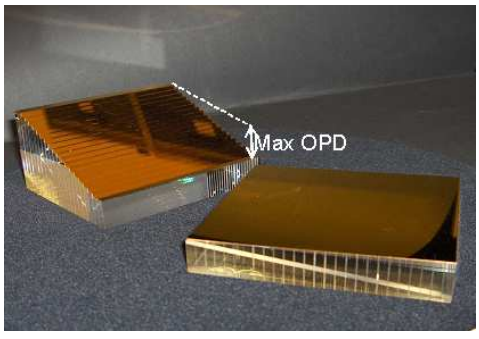

Fig. 2.: prototypes of stepped mirror (CNES R&T).

Each one of the OPD facets corresponds to an interferogram sample. OPD facets are read by imaging them onto a 2D detector array. According to the two stepped mirrors lay-out the interferogram is folded in columns, as shown in Fig. 3:

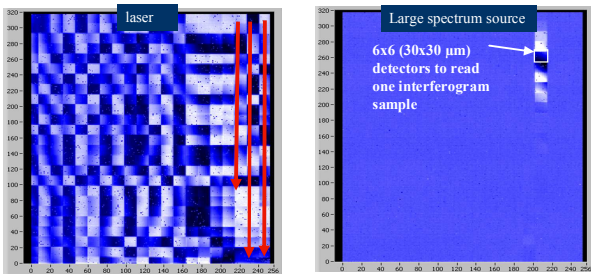

Fig. 3: examples of spatial acquisition of interferograms on a detector matrix (from CNES breadboard). The red arrows show the reading direction of the interferogram.

The technology of mirrors manufacturing based on molecular adherence allows integration of up to one thousand facets in a 100 mm × 100 mm surface. In the frame of SIFTI, the number of interferogram samples is identical to the number of spectral samples due to the acquisition of single side interferograms, sampled according to generalized Shannon criteria. The number of spectral samples is given by $N_S = \frac{\Delta\sigma}{\delta\sigma} = \frac{60}{0.0625} = 960$ Here $\Delta\sigma$ is the spectral width of the spectral narrow filter used to avoid spectral aliasing, as exposed in [2]; $\delta\sigma$ is the spectral sampling step. One can deduce that the minimum need for the interferogram sampling step is $dx = \frac{\max\_OPD}{N_S} = \frac{1}{2.\Delta\sigma} = 83\ \mu m$.

The narrow filter is located in front of the detector. Its spectric transmission has the shape of Fig 4.

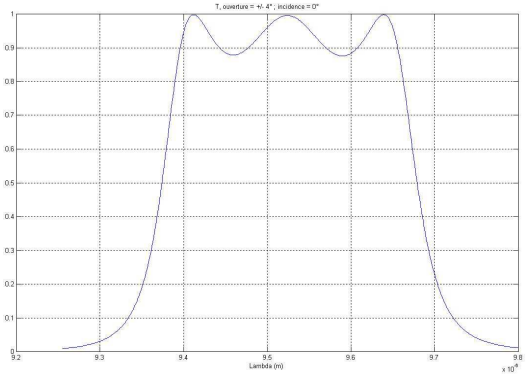

Fig. 4.: Spectric transmission of a 3 cavity filter in B1 band: x axis = wavelength (µm), y axis = normalized transmission.

The filter defines a "useful" bandwidth that must comply with the mission need, i.e. larger than 25 – 30 cm^{-1}, and a "total" bandwidth [σ_{min} ; σ_{max}] to deal with the maximum slop allowed by the technology. Transmission must be close to one in the useful bandwidth, whilst rejection must be near zero outside the total bandwidth, i.e. for wavenumbers inferior to σ_{min} or superior to σ_{max}. Hence the filter technology limitation imposes that the total bandwidth be as twice as large to the useful bandwidth.

2. SIFTI MAIN SPECIFICATIONS

Science objectives and system requirements are presented in details in [1]. The specifications of the data produced by SIFTI are reviewed below.

2.1. Spectral

The spectral band position is determined by the target molecules: O_3 and CO (see Fig. 5). SIFTI spectral band "B1" is dedicated to ozone profile measurement and covers 25 to 30 cm^{-1} in the 1030-1070 cm^{-1} range (about 9.5 µm). SIFTI spectral band "B2" is dedicated to carbon monoxide profile measurement and covers 25 to 30 cm^{-1} in the 2140-2180 cm^{-1} range (about 4.6 µm). Finally, a third band, located in the short-wave infrared domain, will be studied as a possible option: band "B3" dedicated to CO column amount and CH_4, from 4270 to 4300 cm^{-1} (about 2.3 µm).

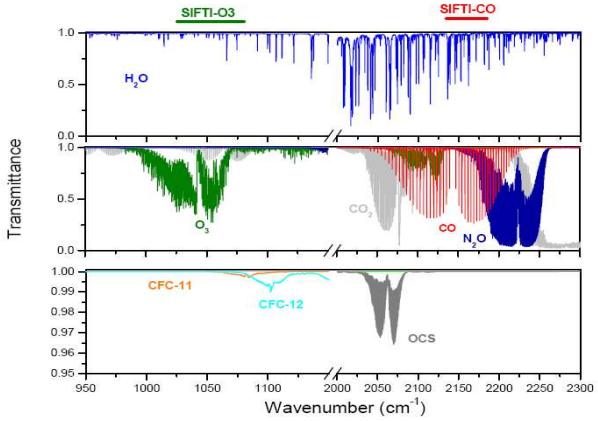

Fig. 5.: main absorbing molecules in the thermal infrared and position of SIFTI spectral bands.

The apodised spectral resolution is 0.125 cm^{-1}, the spectral sampling being $\delta\sigma = 0.0625\ cm^{-1}$.

2.2. Radiometric

The instrument noise requirements are very high too: the Noise Equivalent Difference Temperature (NEDT) at 280 K should be between 0.08 K and 0.13 K for B1, and between 0.13 and 0.2 K for B2 at mission level. Given the presence of pseudo-noises (those that depend

on the homogeneity of the atmospheric target), and of interferogram distortion, the room let for pure radiometric noise yields to a specified Signal to Noise Ratio (SNR) of more than 10^4 in B1 and $3.5.10^3$ in B2, at the level of the interferogram level. This is further discussed in § 5.1.

A fixed pattern distortion criterion was introduced in the interferogram requirements to deal with non temporal noises in it. It is a relative criterion, and it is quite severe. The maximum distortion of the actual interferogram, as compared to the assumed (modeled) interferogram, after quadratic averaging along its samples, is given by Table 1:

	B1 band	B2 band
Around central fringe	10^{-4}	2.10^{-4}
Outside central fringe	4.10^{-5}	8.10^{-5}

Table 1: requirement for the relative index of interferogram distortion

This requirement is equivalent to Instrument Line Shape distortion in a temporal modulating FTS, discussed in the case of IASI in [3]. It is all the more stringent since it includes the effect of knowledge uncertainty of the OPD of the interferogram samples, which must be of the order of few nanometers.

2.3. Geometry

The spatial sampling on ground aims at being 50 km at nadir, and the spatial resolution, i.e. the diameter of the pixel on ground, will be 12 km at nadir. The goal is to obtain at least 25 measurement points in the ±850 km swath.

A powerful option, called "intelligent pointing", would allow the sounder to select, in real time, a zone on the ground to point the pixel at, within an area of 50 km × 50 km (at nadir), according to cloud contamination criteria (either cloud free, or homogeneous). This is symbolized in Fig. 6:

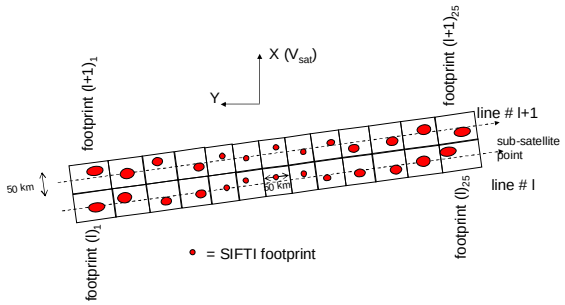

Fig. 6.: Earth scanning with the intelligent pointing option.

The benefit of this intelligent pointing was preliminary studied by CNES, and the results are discussed in the next section.

3. BENEFITS OF INTELLIGENT POINTING

A preliminary study of CMS Météo-France for CNES in 2007 emphasized the benefit of intelligent pointing for a single pixel scanning sounder, like SIFTI. It increases dramatically the occurrence of pointing on cloud free pixels. The cloud mask is based on an already existing algorithm, developed by Meteo France: MAIA [4].

A second study directed by CNES and Météo-France in 2008, has evaluated the sensitivity of cloud detection with respect to degradations in the input data (1 km Spatial Sampling Distance images produced by the embedded imager). This exploratory study was first based on MODIS images, spread over the Earth as shown in Fig. 7. As for the previous study, MAIA has been used as the reference algorithm for cloud detection and identification.

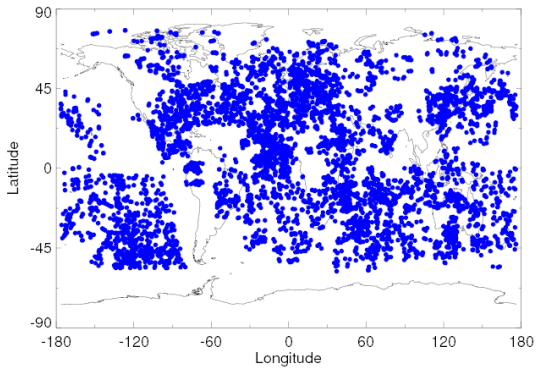

Fig. 7.: location of MODIS images for the study of MAIA tolerances.

Nominally MAIA processes images in 5 spectral bands, from 0.6 µm to 12 µm. But our study demonstrated that, restricted to 2 bands (3.7 µm and 10.8 µm), the efficiency of MAIA remains of great interest, despite the unavoidable degradation of performances: the average rate of non detected clouds rises from 5.6 % to 9.3 % only, the 'earth – day time' situations being the most affected. When an increasing bias error up to 1 K is added to the images, no real degradation is observed on the "MisCloud" criterion. Moreover, addition of noise to the images showed that a NEDT of 0.25 K yields minor degradation. The influence of mis-registration looks low: 1 km mis-registration between the 2 bands lowers the cloud detection efficiency by less than 2 %. This study has led to relaxation of primary requirements for the imager. The present step is the determination of the

best suited spectral bands, TIR bands being preferable for technological reasons (see § 5.6).

A main part of the study consisted in measuring the gain provided to cloud detection, by using real AVHRR images, extracted from 5 orbits of March 15, 2007. According to Table 2, the gain is worthy, even with relaxed specifications of the imager. It can be noticed that the return of the mission could be improved by 50 % thanks to intelligent pointing (assuming that cloudy pixels can not be processed).

Conditions *(% of clouds on considered orbits)*	% of "clear" SIFTI pixels, regular pointing	Gain in % of "clear" SIFTI pixels due to intelligent pointing
Night (*52.5%*)	35%	1.53
Day (*58.4%*)	29.6%	1.42
All orbits (*55%*)	32.8%	1.49

Table 2: statistical results of sounding simulations, on 5 AVHRR orbits of March 15, 2007. A SIFTI pixel is considered as clear if it contains less than 5 % of clouds. Intelligent pointing is simulated with all considered biases (see text)

4. CNES PHASE A STUDY FOR SIFTI

In 2007 CNES started a phase A study for SIFTI, with Thales Alenia Space – France as the prime contractor. The study is divided into two parts. The first one is dedicated to identifying the best technical concept to meet the requirements. Among several solutions, this first approach drew an instrument concept, as suited to insure a satisfactory performance. A description of this preliminary design is given in § 5. The skills and drawbacks of this solution, and the ways forward are discussed in the conclusion

5. INSTRUMENT DESCRIPTION

5.1. Interferometer

From the requirements of § 2, one can deduce the main characteristics of the interferometer.

The maximum OPD must be at least of 8 cm to provide the required spectral sampling. As one on-axis pixel on ground is required, no off axis effect can induce strong apodisation, thus the spectral resolution is weakly affected by the self apodisation of the instrument and the Instrument Line Shape (ILS) is straightforward.

The number of samples in the interferogram, before resampling, is a trade-off between complexity and radiometry. As a matter of fact, more samples would allow to drop the SNR requirement in the interferogram, according to Fig. 8. However, the interferogram SNR requirement is as high as $1.8.10^4$ for 40×40 samples, in B1.

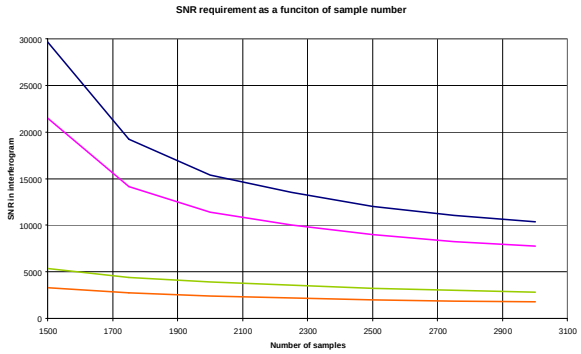

Fig. 8.: SNR requirement in interferogram as a function of samples (before resampling): goal in B1 (blue); threshold in B1 (pink); goal in B2 (green); threshold in B2 (orange).

But numerous samples would increase the complexity of the static interferometer.

Besides, the stepped mirrors hold the aperture pupil of the instrument, so their size is dictated by radiometry. However two considerations might modulate that. The first one is the presence of an afocal telescope of magnitude power of 1.17. It enlarges the pixel Field Of View within the interferometer but reduces the size of its mirrors. The instrument pupil remains the same in front of the telescope. Secondly SIFTI will use a special sampling of the interferogram, made by phase modulating the signal. This is exposed in [5]. This process provides in phase and out of phase samples, with a given set of mirrors. As a consequence, low frequency noises are canceled, so the SNR performance is better.. This yields to stepped mirrors of 77 mm × 77 mm size, forming 24 × 24 facets. The entrance pupil is a square of 90 mm sides. The mechanical step between two consecutive facets is 71 µm. Then a mechanical device, the Phase Modulation Mechanism (PMM) doubles the samples to reach the need dictated by the total spectral bandwidth. It even goes further (1152 samples vs. 960) and the surplus of samples can be used to increase the stability of the resampling algorithm, then to decrease the level of the requirement in Fig. 8.

The PMM consists of wedging the compensator plates and translating them in their plane by 40 µm between two measurements. This changes the apparent OPD in the all pupil, that is to say for all the samples of the interferogram.

5.2. Fore and aft optics

The interferometer is preceded by a scanning mirror, taken up from IASI with slight modifications for pointing agility. It insures the sighting to different targets: the embedded blackbody and the cold space for calibrations, and 25 to 40 footprints along the swath on ground. Then an afocal telescope is used to reduce the input port of the interferometer cavity (settled in the confocal plane), and to reduce the size of the beam coming into the interferometer.

After the interferometer, a mirror focuses the beam to the detection box, and images the earth at its input port as can be seen in Fig. 9.

The main optical bench is regulated at 20° C.

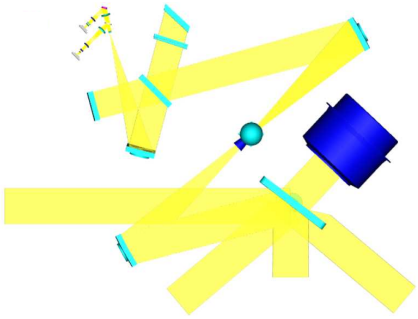

Fig. 9.: SIFTI optical layout.

The cold optics, mounted in the detection box, include a dichroic plate to separate the two bands, two objective lens to image the stepped mirrors on the detectors, and two narrow optical filters.

Introducing the optional SWIR band would require only a second dichroic plate and a dedicated optical path, similar to B1 or B2. B3 detector would take advantage of the cooling for B1 and B2.

5.3. Detectors

Details of the detection subsystem and its cooling system are given by Fig. 10:

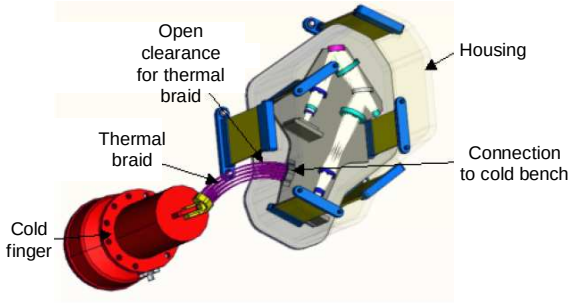

Fig. 10.: detection box and cooling.

A pulse tube cooler cools the detectors to 55 K. The rest of the detection box will be at 200 K. The detectors are commercially available MCT arrays, red in the Integration Then Read mode.

5.4. OPD monitoring

The manufacturing of the steps of the interferometer mirrors insures a positioning accuracy of a few µm. This is not a problem, thanks to the resampling processing, as long as the position of the samples is monitored with a precision of 2 to 5 nanometers. This goal will be achieved by the use of a stabilized laser at 1.54 µm, injected into the interferometer at the level of the confocal point of the entrance telescope, via an integrating sphere. The way back laser beam is read by a commercial 320 × 256 MCT detector array. The accuracy of this device is satisfactory, but it can not deal with too large OPD discrepancies. This is why it is preceded by the processing of the black body measurements themselves, in order to enlarge the range for the mechanical deformations, in the interferometer, that are to be monitored.

5.5. Interferogram processing

The processing of the interferograms of the atmosphere is flanked by views on the calibration targets, i.e. an embedded black body at 20° C, and the cold space. The processing of raw atmospheric interferograms goes through the following steps:

- Non linearity correction
- Phase combination
- Spike detection
- Subtraction of filtered Cold Space interferograms
- AMB
- Pixel merging
- Diffraction correction
- Contrast leveling

The AMB (Atmosphere Minus Blackbody) is an original use of the calibration with a blackbody. By subtracting the signal given by a blackbody to the atmospheric signal, the atmospheric spectral signature is get rid of many instrumental distortions. The blackbody signal has to be previously scaled to fit the radiometric level of the atmosphere. To restore the energetic amplitude of the incoming flux, one has to add a synthetic interferogram, corresponding to the monitored temperature of the blackbody, with the same scaling factor. The AMB method is summarized by the equation below:

$$I_{cor\_atm}(OPD) = I_{raw\_atm}(OPD) - \alpha . I_{measure\_BB}(OPD) \\ \cdots\cdots\cdots\cdots\cdots\cdots + \alpha . I_{Plank}(T_{BB}, OPD)$$

where α is the interferogram envelop maxima ratio between atmosphere and black body.

5.6. Imager integration

The sounder and the CLIM imager will share the same scanning mirror as illustrated by Fig. 11

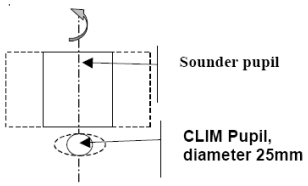

Fig. 11.: projection of the sounder and CLIM imager beams onto the scanning mirror

This optical configuration provides a good registration between the two.

For the imager, a configuration with two thermal infrared (TIR) bands was considered much simpler than one fitting one TIR band and a Medium Wave InfraRed (MWIR) band centered at 3.7 µm. The impact of the TIR – MWIR combination is heavy: an architecture involving only microbolometers can not be proposed and MCT arrays would have be implemented at least for MWIR. This last technology requires cooling devices. Because a thermal machine is not suitable for a small imager, passive cooling must be adapted, but the cold face of the instrument is too far from the imager. Thus, in order to design a very compact imager, it was decided to base the design of CLIM on two microblometer detectors in the TIR. The study presented in § 3 has been extended to forecast the performances of a TIR imager, for cloud detection and classification.

6. INSTRUMENT BUDGET AND PERFORMANCES

Resulting from the above considerations, the preliminary design of the instrument is shown in Fig. 12 and Fig. 13:

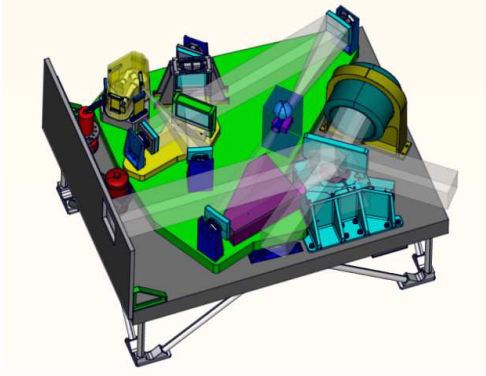

Fig. 12.: SIFTI preliminary design (top view)

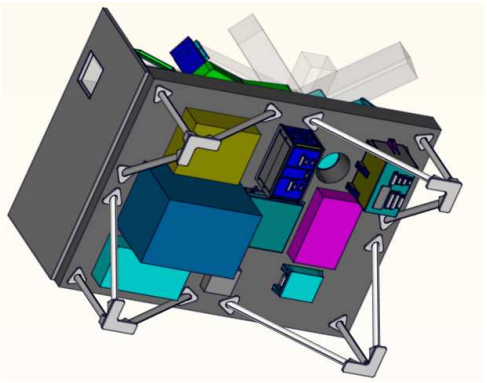

Fig. 13.: SIFTI preliminary design (bottom view)

The structure is of the Vegetation type, with the optical module in the upper cavity, and the electronics under the main mechanical bench. The instrument is self content, no extra parts is needed in the payload module, and its interfaces are simplified.

At this stage of the study, its envelop has the dimensions of Fig. 14:

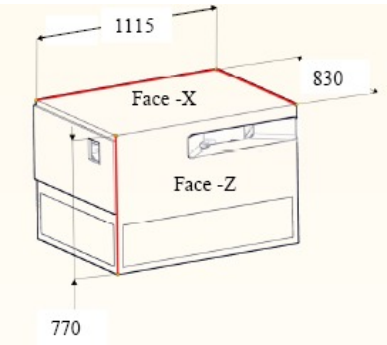

Fig. 14.: SIFTI preliminary size (mm)

The power budget is driven by the cryo cooler. To date it is estimated to more than 300 W, which is to be optimized in the future works.

The mass is 105 kg without margin.

The first radiometric budget is given by Table 3:

	B1 band		B2 band	
	Goal	Threshold	Goal	Threshold
System NEDT requirement (*)	0.08 K	0.13 K	0.13 K	0.2 K
Interferogram SNR requirement	18100	12900	4100	2550
Interferogram SNR performance	19350		3570	
Performance linked to interferogram SNR (*)	0.056 K		0.139 K	
Interferogram distortion performance (*)	0.12 K		0.18 K	
Pseudo noises (*)	0.03 K		0.02 K	
System budget (*)	**0.13 K**		**0.23 K**	

Table 3: first estimation of radiometric performances. (*) = performances converted to NEDT in the spectrum

The four last lines of Table 3 give the system allocation of the main noise items. The most important is linked to the spatial distortion of the interferogram, exposed in § 2.2, as opposed to the temporal noise of the instrument. Globally, it can be seen that the performance is within the need in B1, and marginally out of it in B2.

7. CONCLUSION

The first round in designing an interferometer likely to meet very high performances led to positive results.

First, an instrument concept was found that meets the requirements. It is based on existing technologies, some of them coming from IASI.

Secondly, it was confirmed that such an instrument would be of a great profit to atmospheric science and pollution study. It would bring a new step in this domain.

On the other hand, it appeared that the complexity (for instance: PMM) and the budgets (for instance: power) of such en instrument could be lowered, to remain compatible with low cost or multi sounder missions, in several ways: by using static means for phase modulation, by reducing the size of the interferometer, by using more integrated assembling techniques, or with an improved correction of interferogram distortions. Besides, other detection technologies than MCT could provide a better global trade-off.

This is the reason why a second step of the phase A was decided to implement these solutions in an optimized instrument, and to evaluate the gain they can bring.

At the end of this step, CNES will be in position to make technical choices for a more detailed design. This step by step process should lead to the smallest, less consuming and more simple instrument, whilst providing the required level of performances.

8. REFERENCES

1. Pierangelo C. et al., *SIFTI : a Static Infrared Fourier Transform Interferometer dedicated to ozone and CO pollution monitoring*, International TOVS Study Conference-16, Angra dos Reis, Brasil, 2008.

2. Vermande P. et al., *Spectroscopie par transformée de Fourier des spectres étroits. Application aux interféromètres statiques*., ICSO proceedings, 2000.

3. Blumstein D. et al., *IASI instrument: Technical overview and measured performances,* Infrared spaceborne remote sensing XII conference, proceedings of SPIE, vol. 5543, pp 208-219, 2004.

4. Lavanant L. et al.,: *Operationnal cloud masking for the OSI SAF global METOP/AVHRR SST product*, EUMETSAT meteorological satellite conference, Amsterdam, Netherlands, September 2007.

5. Cansot E. et al., *Static Infrared Fourier Transform Interferometer (SIFTI): benefits of phase modulation processing*, FTS proceedings, 2007.